Security-Enhanced Directional Modulation Symbol Synthesis using High Efficiency Time-Modulated Arrays

Gaojian Huang, *Member, IEEE*, Shufen Chen, Yuan Ding, Xingwang Li, *Senior Member, IEEE*, Arumugam Nallanathan, *Fellow, IEEE*, and Shahid Mumtaz, *Senior Member, IEEE*

***Abstract*—Time-modulated arrays (TMAs) have been found useful to construct directional modulation (DM) transmitters, offering physical-layer security. Two issues, however, exist in conventional TMA DM, which are high power loss and generation of mirror harmonic frequency signals that may compromise wireless security. In this letter, we propose to construct DM transmitters using a high efficiency TMA. By carefully designing the time sequences of the selected phase shifters, the DM symbols modulated upon multicarrier can be synthesized with suppressed mirror harmonic frequencies. It is shown that the proposed TMA DM transmitters here enjoy feeding network efficiency of 100%, and the transmit DM symbols can be synthesized at a pre-selected frequency only, significantly enhancing security performance. The effectiveness of the proposed scheme is validated via bit error rate (BER) simulations. Meanwhile, The TMA DM can also be used as a potential technique for the integrated sensing and communication (ISAC).**

***Index Terms*—Bit error rate (BER), directional modulation (DM), high efficiency, integrated sensing and communication (ISAC), time-modulated array (TMA).**

I. Introduction

DIRECTIONAL modulation (DM) has gained increasing attention owing to its capability of projecting digitally encoded information signals into a pre-specified spatial direction while simultaneously distorting the constellation formats of the same signals in all other directions in free space [1]–[8]. This transmitter end technology originated from the scheme where the near-field electromagnetic (EM) boundary conditions were altered to create direction-dependent data transmissions [2]. Later, at the radio frequency (RF) frontends different DM synthesis approaches were developed, such as by way of optimizing phases of excitation signals in an antenna array [3], [4], or using radiation pattern reconfigurable antenna elements [5]. It was proved in [6] that these RF stage operations could be replaced by operations in digital baseband. In order to simplify the DM hardware implementation, the "synthesis-free" DM concept was proposed, in which the DM transmitter was constructed without calculating the array excitation vectors [7], [8]. Noted that all the above discussed DM works only considered single carrier signals. The authors in [9] were the first to propose a multicarrier orthogonal frequency-division multiplexing (OFDM) DM symbol synthesis approach. However, two associated issues were not discussed, namely high signal peak-to-average power ratio (PAPR) and being not applicable for multiple users. These two issues were subsequently addressed in [10]. The work in [10], on the other hand, raised another concern of the information leakage due to the unintentionally generated signals at mirror harmonic frequencies.

Time-modulated array (TMA) is a technology in which time as a fourth dimension was introduced to antenna array designs [11]. Different to conventional phased arrays, an RF switch is employed to connect or disconnect each antenna element in an array to signal excitation networks. With the help of setting time sequences of connection/disconnection, or ON/OFF in short, the antenna arrays have great flexibility in controlling the aperture excitations, thus the array radiation patterns can be manipulated. This TMA scheme was first proposed for suppressing beampattern sidelobes [11]. Later, it has been found useful in some other applications, such as space division multiple access [12], direction findings [13], and harmonic beamforming [14]–[17]. More recently, TMA was combined with DM concept. For example, in [18] a four-dimensional (4-D) array was presented to achieve DM functionality through the spectrum aliasing effect. In [19], DM was synthesized by way of optimizing the TMA ON/OFF sequences with a binary genetic algorithm. Noted that for the reported TMA DM research works, two issues remain unsolved. One is information leakage due to the unintentionally generated signals at mirror harmonic frequencies, and the other challenge is the low power efficiency because of the energy absorption during switch OFF state in the switch network.

Here in this letter, we propose a security-enhanced DM symbol synthesis approach using high efficiency time-modulated arrays. Comparing with the reference works in [9], [10], the proposed DM architecture can suppress mirror harmonic frequencies and reduce the signal PAPR, resulting in enhanced security performance and higher transmit power efficiency. While comparing with the reference works in [16], [20],

Gaojian Huang, Shufen Chen and Xingwang Li are with the School of Physics and Electronic Information Engineering, Henan Polytechnic University, Jiaozuo 454003, China (e-mails: g.huang@hpu.edu.cn; chenshufen@home.hpu.edu.cn; lixingwangbupt@gmail.com).

Yuan Ding is with the Institute of Sensors, Signals and Systems, Heriot-Watt University, Edinburgh EH14 4AS, U.K. (e-mail: yuan.ding@hw.ac.uk).

Arumugam Nallanathan is with the School of Electronic Engineering and Computer Science, Queen Mary University of London, London E1 4NS, U.K. (e-mail: a.nallanathan@qmul.ac.uk).

Shahid Mumtaz is with the Instituto de Telecomunicacoes, Portugal and Nottingham Trent University, Engineering Department, U.K. (e-mail: smumtaz@av.it.pt).

which focused on shifting energy to sideband, the TMA DM transmitter described in this letter is to synthesize physical-layer secured phase-shift keying (PSK) DM symbols. Moreover, in the proposed TMA DM scheme, multiple access in frequency domain is automatically enabled when the wireless information transmissions to different users are required. The proposed TMA DM therefore can simultaneously generate multiple DM symbol beams at different frequencies, which makes it capable of achieving the integrated sensing and communication (ISAC) functionality. Thus, the proposed TMA DM can be used as a potential technique for the ISAC, a key technology in future wireless systems. The superiorities of the proposed scheme are summarized as follows,

1) The proposed TMA DM can simultaneously generate multiple DM symbol beams at different frequencies along different angular directions, which makes it capable of achieving ISAC functionality. This is in contrast to the suppressing sideband studies in [16], [20];
2) The DM information leakage at the mirror harmonic frequencies can be eliminated. This was not studied in the scheme presented in [10];
3) A feeding network of 100% efficiency can be achieved as RF switches are not configured as OFF state. This is in contrast to that in [9], [10];
4) The signals amplified by power amplifiers (PAs) enjoy 0 dB PAPR since the DM symbols are synthesized via controlling RF switches rather than in baseband domain. This is in contrast to that in [9] where information symbols are synthesized in baseband domain leading to a high PAPR.

The letter is organized as follows. In Section II, the proposed TMA DM transmitter architecture is first described, followed by the multicarrier DM symbol synthesis principle and the evaluation of transmitter system efficiency. In Section III, the effectiveness of the proposed TMA DM scheme is validated and compared with other TMA DM schemes. Finally, conclusions are drawn in Section IV.

II. Proposed TMA DM Transmitters

A. TMA DM Transmitter

In Fig. 1, the architecture of the proposed TMA DM transmitter, consisting of a one-dimensional (1-D) M-element antenna array and a single RF chain as an example is shown. It is assumed that antenna elements are uniformly spaced with $d = \lambda_0/2$ where λ_0 is the wavelength corresponding to the input RF carrier frequency f_0. The amplified input RF signal is first divided into M identical copies by a 1-to-M uniform power splitter. Each signal copy is then phase shifted, the value of which is determined by a single-pole four-throw (SP4T) RF switch, before being radiated through the corresponding antenna element.

It is assumed that the active element pattern of each antenna in the array is identical and isotropic. Thus, the far-field radiation pattern in free space of the TMA shown in Fig. 1 can be expressed as

$$F(\theta) = \frac{e^{j2\pi f_0 t}}{\sqrt{M}} \sum_{m=0}^{M-1} \left(U_m(t) \cdot e^{jm\pi \sin\theta} \right), \quad (1)$$

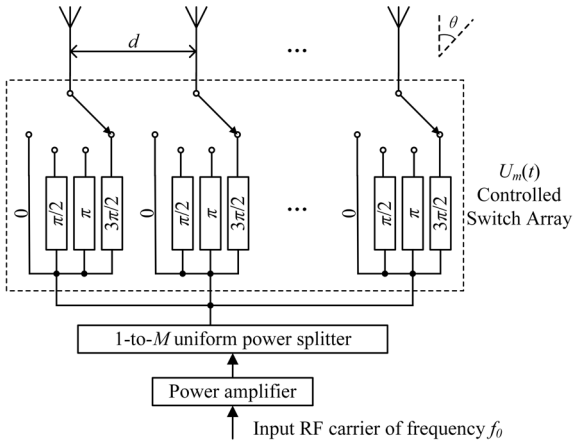

Fig. 1. Proposed TMA DM transmitter architecture.

where θ is the spatial direction relative to the array boresight, seen in Fig. 1, and $\theta \in [-\pi/2, \pi/2]$. $U_m(t)$ refers to the time-domain function describing periodic phase shifting sequences selected by the RF switch in the m^{th} antenna branch. In one time period T_p, in a simplest form we assume that 4 phase shifts are sequentially selected with an identical duration. In a practical scenario, the 4 selectable phase shifters can be realized using low-power SP4T switches which select four signal paths, i.e., transmission lines, with 90° phase difference, and hence it can be written as

$$U_m(t) = \begin{cases} 1 & t_m^s \le t < t_m^s + \frac{1}{4}T_p \\ e^{j\frac{\pi}{2}} & t_m^s + \frac{1}{4}T_p \le t < t_m^s + \frac{1}{2}T_p \\ e^{j\pi} & t_m^s + \frac{1}{2}T_p \le t < t_m^s + \frac{3}{4}T_p \\ e^{j\frac{3\pi}{2}} & t_m^s + \frac{3}{4}T_p \le t < t_m^s + T_p \end{cases}, \quad (2)$$

where t_m^s denotes the switch ON time instants. Since each RF switch is periodically operated, $U_m(t)$ can be expanded into Fourier series as $U_m(t) = \sum_{q=-\infty}^{\infty} c_q \cdot e^{j2q\pi f_p t}$, where $f_p = 1/T_p$, and c_q is the Fourier coefficient for the q^{th} harmonic frequency, which can be expressed as

$$c_q = \begin{cases} \operatorname{sinc}\left(\frac{q}{4}\right) \cdot e^{-j\pi\left(2q\tau_m^s + \frac{q}{4}\right)}, & q = 4i+1 \\ 0\,, & q \ne 4i+1 \end{cases}, i \in Z. \quad (3)$$

Here $\operatorname{sinc}(x) = \sin(\pi x)/\pi x$ and $\tau_m^s = t_m^s/T_p$.

From (3), it can be observed that only when $q = 4i+1$, we have non-zero c_q, which suggests that the indices of harmonic frequencies could only be selected from the set $\{1, -3, 5, -7, 9, \ldots\}$. Thus, the mirror harmonic frequencies are removed when the designed RF switch function in (2) is applied. Noted that for each selectable phase shift, other phase settings can be applied equivalently, for example, $\pi/4$, $3\pi/4$, $5\pi/4$ and $7\pi/4$. In (2), ideally we can sequentially select K identical spaced phase shifts with an identical duration T_p to construct $U_m(t)$, i.e., $U_m(t) = e^{j\frac{2\pi k}{K}}$, $t_m^s + \frac{k}{K}T_p \le t < t_m^s + \frac{k+1}{K}T_p$, $k = 0, 1, \ldots, K-1$. When the number of K increases, more mirror harmonic frequencies will be eliminated, which can be proved using Fourier expansion. However, adding more phase states does not necessarily contribute to

better overall TMA DM systems. For example, more switching states inevitably increase the system complexity, and more importantly, it is usually associated with higher insertion loss. This tradeoff involves more design consideration in hardware implementation, and it is subject to our future study.

Substituting (3) into (1), the radiated signal waveform along θ becomes

$$F(\theta)=\frac{1}{\sqrt{M}}\sum_{q=4i+1,i\in Z}\left(e^{j2\pi(f_0+qf_p)t}\cdot\operatorname{sinc}\left(\frac{q}{4}\right)\cdot\sum_{m=0}^{M-1}e^{j\pi\left(m\sin\theta-2q\tau_m^s-\frac{q}{4}\right)}\right). \tag{4}$$

B. DM Symbol Synthesis

From (4), it can be found that multiple frequencies at f_0+qf_p are generated by the TMA, and we denote radiation pattern at frequency of f_0+qf_p as $F_q(\theta)$. It is assumed that a legitimate user (LU) is located along θ_q in free space. At the LU end, the detected baseband signal at the frequency of f_0+qf_p can be given as

$$F_q(\theta_q)=\frac{\operatorname{sinc}(\frac{q}{4})}{\sqrt{M}}\sum_{m=0}^{M-1}e^{j\pi\left(m\sin(\theta_q)-2q\tau_m^s-\frac{q}{4}\right)}. \tag{5}$$

When $q=1$, i.e., at frequency of f_0+f_p along θ_1, in order to transmit data stream, for instance, binary phase shift keying (BPSK) modulated, two values of τ_m^s expressed as τ_{m1}^s and τ_{m2}^s need to be found out to create two opposite constellation symbols in in-phase and quadrature (IQ) plane, i.e., $F_1(\theta_1)|_{\tau_{m1}^s}$ and $F_1(\theta_1)|_{\tau_{m2}^s}$ where $F_1(\theta_1)|_{\tau_{m1}^s}=-F_1(\theta_1)|_{\tau_{m2}^s}$.

Other data streams could be synthesized onto other frequencies of $q\neq 1$. For instance, two independent data streams can be synthesized at frequencies of f_0+f_p and f_0-3f_p, respectively. In this case, it is assumed that the two data streams are quadrature phase shift keying (QPSK) and BPSK modulated, respectively. Thus, eight possible constellation point combinations $\left[F_1(\theta_1),\ F_{(-3)}(\theta_{(-3)})\right]$, namely $(W_1e^{j\pi/4},\ W_2)$, $(W_1e^{j3\pi/4},\ W_2)$, $(W_1e^{-j\pi/4},\ W_2)$, $(W_1e^{-j3\pi/4},\ W_2)$, $(W_1e^{j\pi/4},\ -W_2)$, $(W_1e^{j3\pi/4},\ -W_2)$, $(W_1e^{-j\pi/4},\ -W_2)$ and $(W_1e^{-j3\pi/4},\ -W_2)$, need to be created, where W_1 and W_2 are complex numbers of the magnitudes which determine the gains towards the directions θ_1 and $\theta_{(-3)}$, respectively. The radiation patterns of $F_1(\theta_1)$ and $F_{(-3)}(\theta_{(-3)})$ can be respectively expressed as

$$F_1(\theta_1)\ =\frac{\operatorname{sinc}(\frac{1}{4})}{\sqrt{M}}\sum_{m=0}^{M-1}e^{j\pi\left(m\sin(\theta_1)-2\tau_m^s-\frac{1}{4}\right)}, \tag{6}$$

and

$$F_{(-3)}(\theta_{(-3)})=\frac{\operatorname{sinc}(-\frac{3}{4})}{\sqrt{M}}\sum_{m=0}^{M-1}e^{j\pi\left(m\sin\left(\theta_{(-3)}\right)+6\tau_m^s+\frac{3}{4}\right)}. \tag{7}$$

To achieve the desired eight constellation point combinations, eight sets of τ_m^s expressed as $\tau_{m1}^s,\ldots,\tau_{m8}^s$ are required. Here, we select particle swarm optimization (PSO) algorithm [14] as an approach example to obtain the solution sets. Using the PSO, to obtain the solution sets, the cost function of τ_m^s needs to be constructed first, followed by setting the parameters in the PSO algorithm such as swarm particle numbers, iteration numbers and initial inertia weight. More example details can be found in Part A of Section III.

It should be noted that in the proposed scheme only one carrier frequency is assigned to a single LU. Multiple frequencies, such as f_0+f_p and f_0-3f_p, can be generated but they are not used for a single user because they will be pointing to different spatial directions. When the proposed scheme is considered for multi-carrier systems, multiple frequencies can be synthesized along the same spatial direction where the LU locates, thus will enable a multi-carrier system.

C. Efficiency Calculation

Different to conventional TMA where the transmit power efficiency is always compromised due to the energy absorption during switch OFF state, in the proposed TMA DM scheme, the overall transmit power efficiency η is only dependent on the harmonic efficiency η_H and feeding network efficiency η_F as PAs have 0 dB of PAPR, thus, we have, $\eta=\eta_H\cdot\eta_F$. Here η_H denotes the harmonic efficiency defined by the ratio of the power of useful harmonics (P_U) to that of all harmonics (P_H), η_F denotes the feeding network efficiency. $P_H=\sum_{q=-\infty}^{+\infty}P_q$, where P_q represents the average radiated power at the q^{th} harmonic frequency which can be given as [21]

$$P_q=4\pi\sum_{m=0}^{M-1}|c_q|^2=4\pi M\operatorname{sinc}^2\left(\frac{q}{4}\right) \tag{8}$$

For better understanding of the transmit power efficiency, as an example, we assume that two harmonic frequencies are used, say f_0+f_p and f_0-3f_p, then P_U can be calculated as

$$P_U=P_1+P_{(-3)}=4\pi\sum_{m=0}^{M-1}|c_1|^2+4\pi\sum_{m=0}^{M-1}\left|c_{(-3)}\right|^2, \tag{9}$$

and P_H is obtained as $4\pi M$ [21]. Since the switch OFF state is eliminated in the proposed TMA DM, we have $\eta_F=100\%$. Thus, in this example, $\eta=90.06\%$. For comparison purpose, considering a single carrier beam, for example, $q=1$, $\eta=81.06\%$, which is higher than the power efficiencies of 30.40%, 32.86%, 40.53% and 49.84% in [22], [10], [15], and [23]. While considering multiple beams, for example, $q=1,-3,5,-7$, the transmit power efficiency will reach a level of 94.95%, which shows similar efficiency performance to that in [16]. Noted that when the number of used harmonic frequencies increases, the power efficiency of the proposed TMA DM can be further improved. Thus the proposed TMA DM enjoys higher transmit power efficiency.

III. Simulation Results

A. DM Symbol Synthesis Examples

In order to validate the effectiveness of the proposed TMA DM scheme, it is assumed that two LUs in free space located at the directions of 45° and -30°, respectively, and $M=9$. In this example, the TMA DM transmitter needs to synthesize two independent data streams delivering to the

TABLE I
QPSK AND BPSK DM SYMBOLS SYNTHESIZED AT FREQUENCIES OF $f_0 + f_p$ AND $f_0 - 3f_p$ ALONG THE DIRECTIONS OF $45°$ AND $-30°$, RESPECTIVELY.

m	τ_{m1}^s	τ_{m2}^s	τ_{m3}^s	τ_{m4}^s	τ_{m5}^s	τ_{m6}^s	τ_{m7}^s	τ_{m8}^s
1	0.77	0.40	0.39	0.04	0.88	0.53	0.20	0.90
2	0.09	0.16	0.46	0.48	0.96	0.98	0.62	0.66
3	0.54	0.20	0.87	0.49	0.37	0.06	0.04	0.70
4	0.94	0.62	0.31	1.00	0.80	0.44	0.43	0.13
5	0.02	0.98	0.64	0.36	0.16	0.91	0.56	0.48
6	0.47	0.15	0.14	0.77	0.63	0.31	0.94	0.63
7	0.90	0.53	0.58	0.19	0.10	0.70	0.45	0.06
8	0.97	0.94	0.61	0.65	0.13	0.13	0.47	0.43
9	0.68	0.39	0.03	0.72	0.51	0.14	0.19	0.88
$F_1(\theta_1)$	$2.04\angle 45°$	$2.04\angle 135°$	$2.04\angle 225°$	$2.04\angle 315°$	$2.04\angle 45°$	$2.04\angle 135°$	$2.04\angle 225°$	$2.04\angle 315°$
$F_{(-3)}(\theta_{(-3)})$	-0.78	-0.78	-0.78	-0.78	0.78	0.78	0.78	0.78
$q = 1$	QPSK 11	QPSK 01	QPSK 00	QPSK 10	QPSK 11	QPSK 01	QPSK 00	QPSK 10
$q = -3$	BPSK 0	BPSK 0	BPSK 0	BPSK 0	BPSK 1	BPSK 1	BPSK 1	BPSK 1

two LUs, e.g., QPSK and BPSK modulated data streams at frequencies of $f_0 + f_p$ and $f_0 - 3f_p$, respectively. This, as we have discussed before, requires eight constellation symbol combinations. Using the PSO algorithm, the cost function can be given as below,

$$\begin{aligned}\text{cost}\left(\tau_m^s\right) = min\left(\omega_1 \cdot \left|F_{o1}(\theta_1, \tau_m^s) - F_{d1}(\theta_1)\right|\right. \\ \left. +\omega_2 \cdot \left|F_{o2}(\theta_2, \tau_m^s) - F_{d2}(\theta_2)\right|\right),\end{aligned} \tag{10}$$

where $F_{ox}\left(\theta_x, \tau_m^s\right)$ (x = 1 or 2) denotes the obtained far-field radiation patterns using optimization algorithm and $F_{dx}\left(\theta_x\right)$ denotes the desired patterns which refer to the patterns with fixed magnitude and phase values for synthesizing QPSK or BPSK symbols. These values will be set according to applied modulation schemes. ω_1 and ω_2 are weighting parameters. One of many possible solution sets of τ_m^s is obtained and shown in Table I.

Setting τ_m^s values according to Table I, the resulting radiation patterns with dB scale and degree scale to depict pattern magnitude and phase are simulated in Figs. 2(a)–(d). In Figs. 2(a) and (c), it can be observed that the beamforming gains are achieved towards the directions of $45°$ and $-30°$, at frequencies of $f_0 + f_p$ and $f_0 - 3f_p$, respectively. Along these two directions, their phase patterns change with fixed values, for example, 0 or π along the direction of $-30°$, seen in Fig. 2(d). While along other directions, the phase patterns are not preserved. Thus, the QPSK and BPSK symbols are synthesized only along the two directions. Noted that the sidelobe level indicates the radiation energy projected along the sidelobe directions. This energy includes the information energy and the artificial interference energy. Thus, it is a trade-off between energy efficiency and transmission secrecy [9].

With the proposed approach, considering a higher order modulation scheme, e.g., eight quadrature amplitude modulation (8QAM), at different harmonic frequency, say $f_0 + 5f_p$ along the direction of $15°$, the radiation patterns are shown in Fig. 3. It can be observed that two different magnitudes are fixed along the direction of $15°$, and each magnitude corresponds to four different phases, thus 8QAM DM symbols are synthesized. Noted that higher order modulations may make the process time consuming because the number of possible constellation symbol combinations across all subcarriers is huge. However, this does not pose limitations on system online operation since this synthesis process can be performed offline.

It can be found that the radiation patterns of proposed TMA DM scheme are synthesized with a constant magnitude and some fixed discrete phases only along the desired direction, while along other directions, the magnitude and phase values

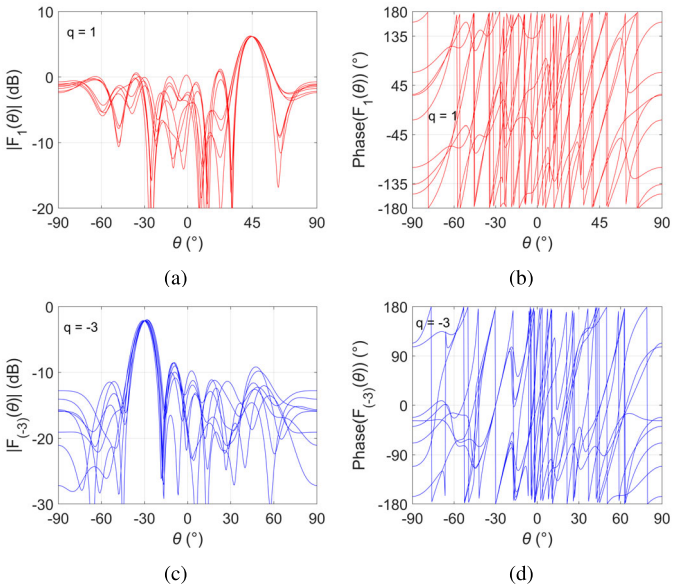

Fig. 2. Far-field radiation patterns. (a), (c) magnitudes in dB; (b), (d) phases in degrees; at frequencies of $f_0 + f_p$, $f_0 - 3f_p$, respectively.

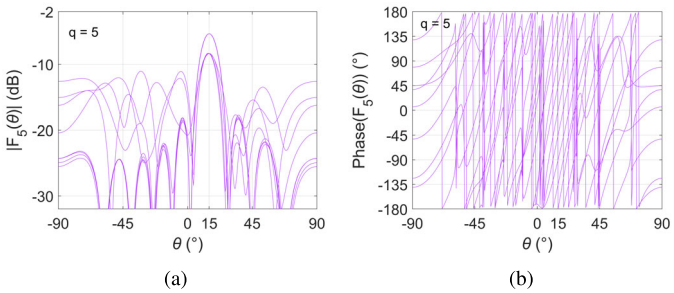

Fig. 3. Far-field radiation patterns. (a) magnitudes in dB; (b) phases in degrees; at frequency of $f_0 + 5f_p$.

of radiation patterns are distorted chaotically. On the contrary in the traditional uniform linear array (ULA) a fixed magnitude and identically spaced phases are preserved along all directions. In the TMA and OFDM-TMA, if no DM function is enabled, the patterns would be similar to those in ULA but with reduced gain due to sideband expansion/leakage. When DM function is added, in the TMA patterns, mirror beams occur that are symmetrical around boresight and in the OFDM-TMA patterns, orthogonal artificial noise is generated and injected in all other directions but with a null towards the desired direction.

B. BER Simulations

In the DM scheme, the security performance of a DM system can be evaluated through different metrics, such as error vector magnitude (EVM)-like metric, secrecy rate, and bit error rate (BER). In [24], it has been concluded that, broadly speaking, all three metrics are equivalent. EVM-like metric is more suitable for static DM, and the calculation of secrecy rate is complicated, and it is more useful to study the link with Gaussian-type modulation. In our proposed scheme, we use QPSK and BPSK as modulation schemes, and the raw BER should be sufficient and appropriate for evaluating the secrecy performance of the link with legitimate receiver along desired direction and potential eavesdroppers in other directions. With this assumption, the BER spatial distribution would illustrate the how secure the information is conveyed to the LU and how much leakage can be expected, e.g., BER sidelobe levels. In all the BER simulations in this letter, we first generate a large number of modulated symbols for transmission, saying 10^{+7}. Since free space transmission is assumed, the symbol streams are added with additive white Gaussian noise (AWGN) at the receiver side, and the noise is assumed to be identical for receivers located along all directions (this is for BER spatial distribution simulations). The amount of the noise power is weighted to scale the signal-to-noise ratio (SNR) along the secure communication direction to a pre-set value. By using this Monte Carlo simulation, the security performance of the proposed DM system can be fully depicted by the BER spatial distribution simulations, where high BER sidelobes indicate poor security performance.

In Fig. 4, the BERs of the proposed TMA DM have been simulated and shown with the value of τ_m^s being configured according to Table I. It is assumed that SNRs are respectively set to 10 dB and 15 dB to better illustrate the BER differences, especially sidelobe levels, between the corresponding ULAs and the DM arrays. Different SNRs are equivalent to setting different distances between the transmitter and receivers that include the LU along θ_q and potential eavesdroppers along all other directions. It can be observed that at frequencies of $f_0 + f_p$ and $f_0 - 3f_p$, the BER main beams of the proposed scheme are focused along the directions of $45°$ and $-30°$, respectively. While along other directions, the BERs have low sidelobes which suggests that information cannot be intercepted along these directions. In Fig. 4, the BERs of the conventional phased array, which is also named as ULA in this letter, are simulated. In Fig. 4(a), the BERs of a conventional ULA with applied QPSK (for beamforming direction of $45°$) and BPSK (for beamforming direction of $-30°$) modulations are depicted at SNR level of 10 dB. It is observed that high BER sidelobe levels occur, which indicates information can be easily intercepted along these angular directions. These high BER sidelobe levels will be further increased at higher SNR, for example 15 dB, seen in Fig. 4(b). Thus, when the SNR values increase, higher BER sidelobe levels are present in the ULA schemes, resulting in a poor security performance. While in the proposed TMA DM scheme, the BER sidelobe levels are sufficiently suppressed, indicating that information can hardly be intercepted along these directions whatever at high or low SNR levels.

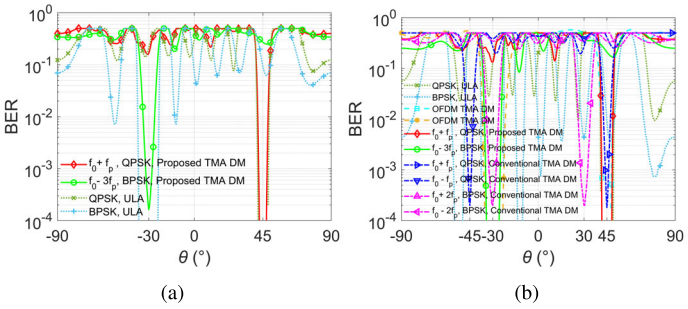

Fig. 4. The BERs of various DM schemes. (a) SNR=10dB. (b) SNR=15dB.

From the comparison results of various DM schemes are illustrated in Fig. 4(b). It can be observed that in conventional TMA DM [10] the BER main beams of mirror harmonic frequencies are symmetrical with respect to the direction of $0°$. This would result in information leakage as confidential information can be intercepted by an eavesdropper along the directions of $-45°$ or $30°$, posing security threat. While in the proposed TMA DM scheme, the mirror harmonic frequencies are eliminated, thus only along the LU direction, a BER main beam can be obtained. For example, along the desired secure communication direction of $45°$. It can be observed that the proposed TMA DM only has a single BER main beam along the desired direction of $45°$, and along other directions has low BER values, indicating that information can hardly be intercepted in other directions except the desired direction. Meanwhile, the OFDM DM scheme in [9] can secure information but with a high PAPR issue.

In this letter, we focused on enhancing the TMA DM security performance. In conventional TMA DM schemes, the eavesdroppers can intercept information leaked along the directions where the mirror harmonics locate. To address this issue, it requires non-symmetrical switching functions, which, unfortunately, reduce the available subcarrier numbers. This trade-off is inherent in TMA systems, and it demands further study in this area. Usually, only a limited number of carrier frequencies are used in a TMA due to suppressed power of high-order harmonic frequencies. Noted that when the proposed scheme is considered for ISAC systems, it is assumed that the transmitter and receiver are co-located, and the target positions are to be estimated. Different with the conventional DM, here the synthesized DM beams will be scanning in the angular domain with the help of changing

the time sequences of the switching functions. The detected BER of backscattering signals will drop to a very low value only when the beam scanning direction aligns with the target direction. In this way the unknown targets can be localized and tracked, and when the target equips with a suitable receiver, information can be delivered to the target.

IV. Conclusion

In this letter, a novel TMA structure was developed to achieve DM functionality. It has been shown that the proposed TMA DM scheme can achieve a feeding network efficiency of 100%, and importantly, the issue of information leakage through signals generated by a conventional TMA at mirror harmonic frequencies is addressed since in the proposed TMA DM the mirror harmonic frequencies are suppressed. Therefore, the proposed TMA DM not only integrates the benefits of conventional TMA DM, such as single RF chain, 0 dB PAPR and multiple access enabled in frequency domain, but also with higher power efficiency and enhanced security performance. Moreover, the multi-beams synthesized here are able to deliver secure wireless communication to a target and simultaneously sensing other targets.

References

[1] Y. Ding and V. Fusco, "A vector approach for the analysis and synthesis of directional modulation transmitters," *IEEE Trans. Antennas Propag.*, vol. 62, no. 1, pp. 361–370, Jan. 2014.
[2] A. Babakhani, D. B. Rutledge, and A. Hajimiri, "Transmitter architectures based on near-field direct antenna modulation," *IEEE J. SolidState Circuits*, vol. 43, pp. 2674–2692, 2008.
[3] A. Babakhani, D. Rutledge, and A. Hajimiri, "Near-field direct antenna modulation," *IEEE Microw. Mag.*, vol. 10, no. 1, pp. 36–46, Feb. 2009.
[4] M. P. Daly and J. T. Bernhard, "Directional modulation technique for phased arrays," *IEEE Trans. Antennas Propag.*, vol. 57, no. 9, pp. 2633–2640, Sep. 2009.
[5] M. P. Daly and J. T. Bernhard, "Beamsteering in pattern reconfigurable arrays using directional modulation," *IEEE Trans. Antennas Propag.*, vol. 58, no. 7, pp. 2259–2265, Jul. 2010.
[6] A. Kalantari, M. Soltanalian, S. Maleki, S. Chatzinotas, and B. Ottersten, "Directional modulation via symbol-level precoding: A way to enhance security," *IEEE J. Sel. Topics Signal Process.*, vol. 10, no. 8, pp. 1478–1493, Dec. 2016.
[7] N. N. Alotaibi and K. A. Hamdi, "Switched phased-array transmission architecture for secure millimeter-wave wireless communication," *IEEE Trans. Commun.*, vol. 64, no. 3, pp. 1303–1312, Mar. 2016.
[8] Y. Ding and V. Fusco, "A synthesis-free directional modulation transmitter using retrodirective array," *IEEE J. Sel. Topics Signal Process.*, vol. 11, no. 2, pp. 428–441, Mar. 2017.
[9] Y. Ding, V. Fusco, J. Zhang, and W. Wang, "Time-modulated OFDM directional modulation transmitters," *IEEE Trans. Veh. Technol.*, vol. 68, no. 8, pp. 8249–8253, Aug. 2019.
[10] G. Huang, Y. Ding and S. Ouyang, "Multicarrier directional modulation symbol synthesis using time-modulated phased arrays," *IEEE Antennas Wireless Propag. Lett.*, vol. 20, no. 4, pp. 567–571, Apr. 2021.
[11] W. Kummer, A. Villeneuve, T. Fong and F. Terrio, "Ultra-low sidelobes from time-modulated arrays," *IEEE Trans. Antennas Propag.*, vol. 11, no. 6, pp. 633–639, Nov. 1963.
[12] C. He, X. L. Liang, B. Zhou, J. P. Geng, and R. H. Jin, "Space-division multiple access based on time-modulated array," *IEEE Antennas Wireless Propag. Lett.*, vol. 14, pp. 610–613, 2015.
[13] G. Ni, C. He, J. Chen, L. Bai and R. Jin, "Direction finding and performance analysis with 1 bit time modulated array," *IEEE Trans. Antennas Propag.*, vol. 69, no. 10, pp. 6881–6893, Oct. 2021.
[14] L. Poli, P. Rocca, G. Oliveri, and A. Massa, "Harmonic beamforming in time-modulated linear arrays," *IEEE Trans. Antennas Propag.*, vol. 59, no. 7, pp. 2538–2545, Jul. 2011.
[15] H. Li, Y. Chen and S. Yang, "Harmonic beamforming in antenna array with time-modulated amplitude-phase weighting technique," *IEEE Trans. Antennas Propag.*, vol. 67, no. 10, pp. 6461–6472, Oct. 2019.
[16] R. Maneiro-Catoira, J. A. Garcła-Naya, J. Brgains, and L. Castedo, "Multibeam single-sideband time-modulated arrays," *IEEE Access*, vol. 8, pp. 151976–151989, Aug. 2020.
[17] U. Yesilyurt, I. Kanbaz, S. Kuzu and E. Aksoy, "A Noniterative Convoluted Harmonic Beamforming Technique in Time Modulated Arrays," *IEEE Trans. Antennas Propag.*, vol. 69, no. 2, pp. 795–805, Feb. 2021.
[18] Q. Zhu, S. Yang, R. Yao and Z. Nie, "Directional modulation based on 4-D antenna arrays," *IEEE Trans. Antennas Propag.*, vol. 62, no. 2, pp. 621–628, Feb. 2014.
[19] J. Guo, L. Poli, M. A. Hannan, P. Rocca, S. Yang and A. Massa, "Time-modulated arrays for physical layer secure communications: optimization-based synthesis and experimental assessment," *IEEE Trans. Antennas Propag.*, vol. 66, no. 12, pp. 6939–6949, Dec. 2018.
[20] Y. Gao et al., "Single-sideband time-modulated phased array with 2-bit phased shifters," in *Proc. 9th Asia–Pacific Conf. Antennas Propag. (APCAP)*, Xiamen, China, Aug. 2020, pp. 1–2.
[21] R. Maneiro-Catoira, J. C. Brgains, J. A. Garcła-Naya, L. Castedo, P. Rocca and L. Poli, "Performance analysis of time-modulated arrays for the angle diversity reception of digital linear modulated signals," *IEEE J. Sel. Topics Signal Process.*, vol. 11, no. 2, pp. 247–258, Mar. 2017.
[22] A. Yao, W. Wu and D. Fang, "Single-sideband time-modulated phased array," *IEEE Trans. Antennas Propag.*, vol. 63, no. 5, pp. 1957–1968, May. 2015.
[23] R. Maneiro-Catoira, J. Brgains, J. A. Garcła-Naya and L. Castedo, "Time-modulated arrays with Haar wavelets," *IEEE Antennas Wireless Propag. Lett.*, vol. 19, no. 11, pp. 1862–1866, Nov. 2020.
[24] Y. Ding and V. Fusco, "Establishing metrics for assessing the performance of directional modulation systems," *IEEE Trans. Antennas Propag.*, vol. 62, no. 5, pp. 2745–2755, Feb. 2014.